PROCEEDINGS OF SCIENCE

Event-by-event jet suppression, anisotropy and hard-soft tomography

Yayun He*
Key Laboratory of Quark and Lepton Physics (MOE) and Institute of Particle Physics, Central China Normal University, Wuhan 430079, China
E-mail: heyayun@mails.ccnu.edu.cn

Shanshan Cao
Department of Physics and Astronomy, Wayne State University, Detroit, Michigan 48201, USA

Wei Chen
Key Laboratory of Quark and Lepton Physics (MOE) and Institute of Particle Physics, Central China Normal University, Wuhan 430079, China

Tan Luo
Key Laboratory of Quark and Lepton Physics (MOE) and Institute of Particle Physics, Central China Normal University, Wuhan 430079, China

Long-Gang Pang
Physics Department, University of California, Berkeley, California 94720, USA
Nuclear Science Division Mailstop 70R0319, Lawrence Berkeley National Laboratory, Berkeley, CA 94740,USA

Xin-Nian Wang
Key Laboratory of Quark and Lepton Physics (MOE) and Institute of Particle Physics, Central China Normal University, Wuhan 430079, China
Physics Department, University of California, Berkeley, California 94720, USA
Nuclear Science Division Mailstop 70R0319, Lawrence Berkeley National Laboratory, Berkeley, CA 94740,USA

In heavy-ion physics, the inclusive jet suppression and anisotropy are studied within the Linear Boltzmann Transport(LBT) model. Both agree well with experimental results from Large Hadron Collider (LHC) experiments. The inclusive jet suppression factor is found to depend on the initial jet spectrum and jet quenching. With event-by-event fluctuating hydrodynamic simulations, an approximately linear correlation is found between jet azimuthal anisotropy and the bulk azimuthal anisotropy.

International Conference on Hard and Electromagnetic Probes of High-Energy Nuclear Collisions
30 September - 5 October 2018
Aix-Les-Bains, Savoie, France

*Speaker.

PoS(HardProbes2018)100

1. Introduction

In high energy heavy ion collisions, a unique state of matter called quark-gluon plasma (QGP) is created at the Relativistic Heavy-Ion Collider (RHIC) [1, 2] and the Large Hadron Collider (LHC) [3]. High-p_T partons produced in the early stage of these collisions traverse the QGP and interact with a strength described by the jet transport coefficient $\hat{q}/T^3 \approx 4-8$ [4]. Given such strong interaction, the energy deposited into the medium by jets is considerable and leads to high jet suppression compared to jet transport in the vacuum. The inclusive jet suppression factor has been measured in Pb+Pb collisions at both $\sqrt{s} = 2.76$ TeV and $\sqrt{s} = 5.02$ TeV at LHC [5, 6, 7]. A weak p_T dependence is observed at high p_T and the suppression factor has almost the same value at the two energies, although the bulk density at the mid-rapidity region at $\sqrt{s} = 5.02$ TeV increases by about 20% with respect to the lower energy [8, 9] and a larger suppression is expected. On the other hand, the expanding medium shows asymmetry in momentum space due to the asymmetry in configuration space in non-central nucleus-nucleus collisions, which implies that jet quenching depends on the jet direction with respect to the reaction plane, and jet anisotropy arises. Jet anisotropy also correlates with the final bulk anisotropy since both of them are dependent on the initial fluctuating energy density distribution during the hydrodynamic expansion. This study is aimed to describe both jet suppression and anisotropy in a unified framework.

2. The LBT model

The Linear Boltzmann Transport (LBT) model [10, 11, 12, 13] is based on the Boltzmann equation including both elastic scattering and inelastic scattering. The elastic scattering rate is calculated according to the leading order perturbative Chromodynamics (pQCD), while the inelastic scattering rate is extracted from a next-to-leading order twist-4 approach [14, 15]. The elastic probability and inelastic probability in each time step obey Poisson distribution, and they are implemented to ensure unitarity. The only adjustable parameter in the LBT model is the strong coupling constant $\alpha_s = 0.15$, which is an effective coupling constant to describe the strong interaction regulated by a Debye screening mass.

The LBT model allows the re-scattering for jet shower partons, jet-induced medium recoils and radiated gluons. It also includes the jet-induced medium back reaction which is denoted as "negative" particles since the four momenta of which are subtracted during final jet reconstruction with anti-k_t algorithm to ensure the global energy-momentum conservation. The initial jet shower partons are generated by PYTHIA 8, and the medium information such as initial geometry, local temperature and fluid velocity is provided by the (3+1)D CLVisc hydrodynamic model [16, 17]. The model has a linear approximation and is only valid if the density of the medium excitation is much smaller than the medium density. For validation of a more general situation. a coupled LBT and hydrodynamic (CoLBT-hydro) model is developed [18], in which the deposited energy of the jet shower partons is input as a source term of the hydrodynamic evolution in real time.

3. The inclusive jet suppression and anisotropy

First we should provide the validation of the initial jet spectrum. In Fig. 1 we show the jet cross section differential in p_T and y with jet cone size $R = 0.4$ at both $\sqrt{s} = 2.76$ TeV and $\sqrt{s} = 5.02$

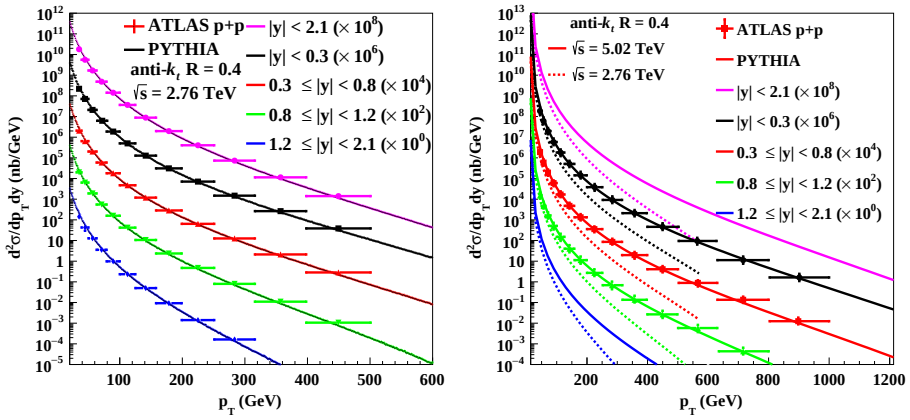

Figure 1: (Color online) The inclusive jet double differential cross section as a function of jet p_T in different rapidity bins in p+p collisions using anti-k_t algorithm with jet radius $R = 0.4$ from PYTHIA 8 compared to ATLAS experimental data. Results for different rapidity bins are scaled by successive power of 10^2. (Left) $\sqrt{s} = 2.76$ TeV (solid lines); (right) $\sqrt{s} = 2.76$ TeV (dash lines) and $\sqrt{s} = 5.02$ TeV (solid lines).

TeV in p+p collisions. Results from PYTHIA 8 can well describe the experimental data [5, 6]. In Fig. 1 (right) one can see that the spectrum at $\sqrt{s} = 5.02$ TeV is much flatter than at $\sqrt{s} = 2.76$ TeV, which originates from the difference of parton distribution functions at different colliding energies.

After we get the baseline in p+p collisions, we can calculate the inclusive jet suppression factor. Fig. 2 (left) shows the p_T dependence of the averaged jet p_T loss at $\sqrt{s} = 5.02$ TeV and $\sqrt{s} = 2.76$ TeV. One can see there is indeed an about 11% enhancement of energy loss at the higher colliding energy. However, as seen in Fig. 2 (right) the jet suppression factors at both colliding energies have a weak p_T dependence at high p_T and they are almost the same in both experimental data and calculations. Apart from the p_T dependence of the energy loss, the deciding contribution to jet R_{AA} is the initial jet spectrum in p+p collisions. One can see that in Fig. 1 (right) the spectrum gets much flatter as jet p_T increases and the spectrum at $\sqrt{s} = 5.02$ TeV is flatter than at $\sqrt{s} = 2.76$ TeV. The flatness of jet p_T spectrum competes with the p_T dependence of jet energy loss and give a weak p_T dependence of jet R_{AA}.

To make an estimate, one can calculate jet R_{AA} according to Eq. (3.1),

$$R_{AA}(p_T) \approx \frac{d\sigma^{jet}_{p+p}(p_T + \langle \Delta p_T \rangle)}{d\sigma^{jet}_{p+p}(p_T)}. \tag{3.1}$$

Here jet R_{AA} at a given jet p_T approximately equals the ratio of shifted differential cross section at that p_T plus the averaged p_T loss over the original differential cross section at the jet p_T. And the shifted jet R_{AA} shown as the dashed lines in Fig. 2 (right) gives a consistent description of the experimental data.

After the shape of the inclusive jet suppression is figured out, we calculate jet azimuthal anisotropy in the same framework according to scalar product method as Eq. (3.2) (left) and event

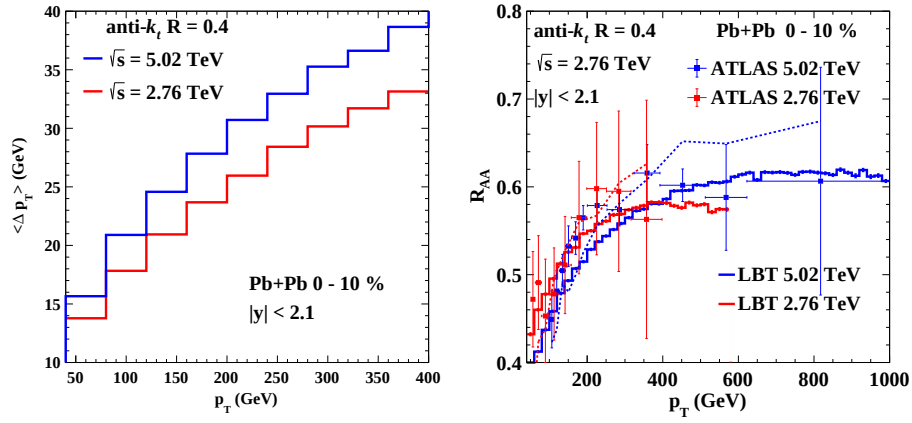

Figure 2: (Color online) p_T dependence of the averaged jet p_T loss (left) and the inclusive jet suppression factor R_{AA} (right) with jet radius $R = 0.4$ at $\sqrt{s} = 5.02$ TeV (blue) and $\sqrt{s} = 2.76$ TeV (red) at Pb+Pb collisions at $0-10\%$ centrality in jet rapidity $|y| < 2.1$. The dashed lines are suppression factors obtained by shifting the $p+p$ spectrum by the averaged p_T loss according to Eq. (3.1).

plane method as Eq. (3.2) (right),

$$v_2^{jet} = \frac{\langle\langle v_2^{soft} \cos(2[\phi^{jet} - \Psi_2])\rangle\rangle}{\sqrt{\langle\langle (v_2^{soft})^2\rangle\rangle}}, \qquad v_2^{jet} = \langle\langle \cos(2[\phi^{jet} - \Psi_2])\rangle\rangle. \tag{3.2}$$

The two methods are denoted as "LBT w. fluc." (solid) and "LBT w/o fluc." (dash) respectively in Fig. 3 (left) and the results of both are almost the same due to the distributions of the bulk v_2. The jet azimuthal anisotropy at $\sqrt{s} = 2.76$ TeV agrees well with the experimental data [19] and is comparable with that at $\sqrt{s} = 5.02$ TeV, which is consistent with jet R_{AA}. In Fig. 3 (right) one can see there is an approximately linear correlation between the jet azimuthal anisotropy and bulk azimuthal anisotropy. Such hard-soft correlation can be ascribed to the initial energy density fluctuation and jet quenching.

4. Conclusion

The inclusive jet suppression is not only dependent on jet quenching, but also largely influenced by the initial jet spectrum. And the LBT model is capable to describe the jet suppression and jet azimuthal anisotropy in a unified framework. One also finds that the hard-soft correlation is approximately linear.

5. Acknowledgement

This work is supported by the NSFC under grant No. 11521064, NSF within the JETSCAPE Collaboration and under grant No. ACI-1550228, and ACI-1550300, and U.S. DOE under Contract Nos. DE-AC0205CH11231 and DE-SC0013460. Computations are performed at the Green Cube at GSI, GPU workstations at CCNU and the DOE NERSC.

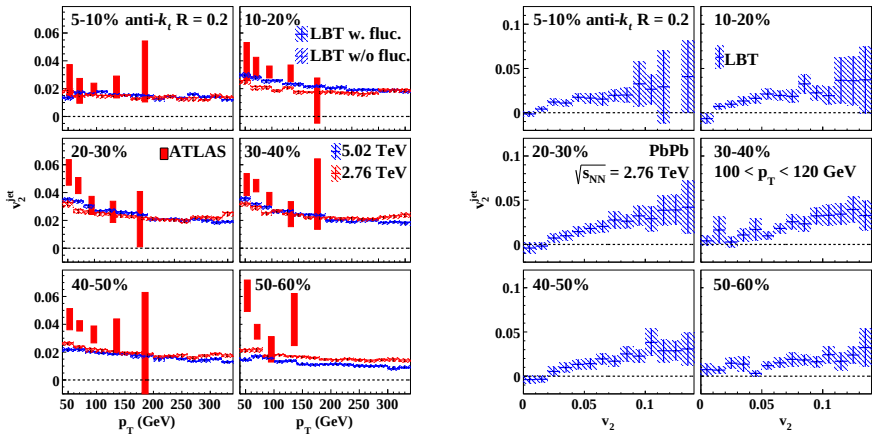

Figure 3: (Color online) (left)p_T dependence of jet azimuthal anisotropy v_2^{jet} with jet radius $R = 0.2$ at $\sqrt{s} = 2.76$ TeV (red) and $\sqrt{s} = 5.02$ TeV (blue) at different centrality bins with (solid) or without (dashed) fluctuating bulk v_2, compared to experimental data at $\sqrt{s} = 2.76$ TeV (red boxes); (right) Hard-soft correlation between jet azimuthal anisotropy and bulk azimuthal anisotropy with jet radius $R = 0.2$ at $\sqrt{s} = 2.76$ TeV at different centrality bins.

References

[1] STAR Collaboration, *Nucl. Phys. A* **757**, 102 (2005).

[2] PHENIX Collaboration, *Nucl. Phys. A* **757**, 184 (2005).

[3] B. Muller, J. Schukraft, and B. Wyslouch, *Annu. Rev. Nucl. Part. Sci.* **62**, 361 (2012).

[4] JET Collaboration, *Phys. Rev. C* **90**, no. 1, 014909(2014).

[5] ATLAS Collaboration, *Phys. Rev. Lett.* **114**, 072302 (2015).

[6] ATLAS Collaboration, (2018), [arXiv:1805.05635].

[7] CMS Collaboration, *Phys. Rev. C* **96**, 015202 (2017).

[8] ALICE Collaboration, *Phys. Lett. B* **726**, 610 (2013).

[9] ALICE Collaboration, *Phys. Lett. B* **772**, 567 (2017).

[10] H. Li, F. Liu, G. l. Ma, X. N. Wang and Y. Zhu, *Phys. Rev. Lett.* **106**, 012301 (2011).

[11] X. N. Wang and Y. Zhu, *Phys. Rev. Lett.* **111**, no. 6, 062301 (2013).

[12] Y. He, T. Luo, X. N. Wang and Y. Zhu, *Phys. Rev. C* **91**, 054908 (2015) Erratum:[*Phys. Rev. C* **97**, no. 1, 019902 (2018)].

[13] S. Cao, T. Luo, G. Y. Qin and X. N. Wang, *Phys. Lett. B* **777**, 255 (2018).

[14] X. F. Guo and X. N. Wang, *Phys. Rev. Lett.* **85**,3591 (2000).

[15] X. N. Wang and X. F. Guo, *Nucl. Phys. A* **696**, 788 (2001).

[16] L. G. Pang, Q. Wang and X. N. Wang, *Phys. Rev. C* **86**, 024911 (2012).

[17] L. G. Pang, H. Petersen and X. N. Wang, *Phys. Rev. C* **97**, no. 6, 064918 (2018).

[18] W. Chen, S. Cao, T. Luo, L. G. Pang and X. N. Wang, *Phys. Lett. B* **777**, 86 (2018).

[19] ATLAS Collaboration, *Phys. Rev. Lett.* **111** 152301 (2013).